

Oxide Ion Conductivity and Chemical Stability of Lanthanum Fluorides Doped with Oxygen, $\text{La}(\text{Sr},\text{Na})\text{F}_{3-2x}\text{O}_x$

Masaki Ando,[‡] Makiko Enoki,^{‡,§} Hiroyasu Nishiguchi,[†] Tatsumi Ishihara,^{*,†,§} and Yusaku Takita[†]

Department of Applied Chemistry, Faculty of Engineering, and Materials Production Course, Graduate School of Engineering, Oita University, Dannoharu 700, Oita 870-1192, Japan

Received May 21, 2004. Revised Manuscript Received June 19, 2004

Oxide ion conductivity in doped $\text{LaO}_x\text{F}_{3-2x}$ was investigated. It was found that oxygen doped into LaF_3 can be mobile through introduced anion vacancy and $\text{LaO}_{0.6}\text{F}_{1.8}$ exhibits the high oxide ion conductivity, which is comparable with those in doped Bi_2O_3 -based oxides. The oxide ion conductivity in $\text{LaO}_{0.6}\text{F}_{1.8}$ was further improved by simultaneous doping of SrO , SrF_2 , and NaF . The highest conductivity is achieved with the composition $\text{La}_{0.9}\text{Sr}_{0.1}\text{Na}_{0.05}\text{O}_{0.4}\text{F}_{2.0}$ in the present study. $\text{La}_{0.9}\text{Sr}_{0.1}\text{Na}_{0.05}\text{O}_{0.4}\text{F}_{2.0}$ is chemically stable in oxygen partial pressure from 1 to 10^{-21} atm, and almost the theoretical electromotive force is exhibited in the oxygen gas-concentration cell. The conductivity of oxygen-doped LaF_3 was further confirmed by the dc polarization method. No polarization in conductivity was observed over 24 h, and also no segregation of F^- ion at positive electrode was noticed. Furthermore, desorption of F_2 from lattice was not observed. Therefore, it was confirmed that oxygen-doped LaF_3 exhibits oxide ion conductivity. The chemical stability of $\text{La}_{0.9}\text{Sr}_{0.1}\text{O}_{0.4}\text{F}_{2.0}$ was further studied, and it was confirmed that F-rich lanthanum oxyfluoride is highly stable against humidity not only at elevated but also at room temperature.

Introduction

The conventional fast oxide ion conductor so far has been based on pure metal oxides with oxygen defects.¹ Particularly, tetravalent metal oxides with the fluorite structure, doped with lower valence cations, are well-known as oxide ion conductor.² For example, zirconium oxide doped with Y_2O_3 or Sc_2O_3 is generally used for the electrolyte of fuel cells and oxygen sensors. However, in the case of the high oxide ion conductors of CeO_2 or Bi_2O_3 , the material becomes unstable and reduction easily proceeds to generate electronic conduction. So, the oxygen partial pressure range for which oxide ion conductivity dominates becomes narrower with the increased oxide ion conductivity among the fluorite structured oxides.³ It is also well-known that Bi_2O_3 doped with Y_2O_3 exhibits high oxide ion conductivity; however, this oxide can be used as the oxide ion conductor only in the limited P_{O_2} range, due to reduction.⁴ Except for fluorite structured oxide ion conductors

such as ZrO_2 , CeO_2 , and Bi_2O_3 , the number of fast oxide ion conductor is limited until now. Recently, several new fast oxide ion conductors such as LaGaO_3 ,⁵ $\text{La}_{10}\text{Si}_6\text{O}_{27}$,^{6,7} and La_2GeO_5 ⁸ were reported. However, all of these materials are also metal oxides with oxygen deficiency. The most promising application of these oxide ion conductors is for the electrolyte of fuel cells. In fact, the operating temperature of the solid oxide fuel cells could decrease to 873 from 1273 K by changing the electrolyte from $\text{Y}_2\text{O}_3\text{--ZrO}_2$ to $\text{La}(\text{Sr})\text{Ga}(\text{Mg})\text{O}_3$.⁹ From the viewpoint of electrolyte application, oxide ion conductors are required not only with high oxide ion conductivity but also high chemical stability.⁹

Studies on the oxide ion conductivity in metal oxyfluoride ($\text{M}(\text{III})\text{OF}$; $\text{M}(\text{III})$ = trivalent metal cation) and/or metal fluoride ($\text{M}(\text{III})\text{F}_3$) is limited until now. In particular, oxide ion conductivity in metal fluoride doped with oxygen was not studied yet. Takashima et al. investigated the oxide ion conductivity in the various double cation oxyfluorides ($\text{MM}'\text{O}_2\text{F}_6$, M, M' : trivalent metal cations), and they found that $\text{Nd}_2\text{--Eu}_2\text{O}_3\text{F}_6$ exhibits high oxide ion conductivity (oxide

* To whom correspondence should be addressed. Fax: +81-92-642-3551. E-mail: ishihara@cstf.kyuhu-u.ac.jp.

[†] Department of Applied Chemistry.

[‡] Graduate School of Engineering.

[§] Present address: Department of Applied Chemistry, Faculty of Engineering, Kyushu University, Hokozaeki 6-10-1, Higashi-Ku, Fukuoka, 812-8581, Japan.

(1) Minh, N. Q.; Takahashi, T. *Science and Technology of Ceramic Fuel Cells*; Elsevier: New York, 1995; pp 69–107.

(2) Choudhary, C. B.; Maiti, H. S.; Subbarao, E. C. *Defects Structure and Transport Properties. Solid State Electrolytes and Their Applications*; Plenum Press: New York, 1980; pp 1–68.

(3) Goodenough, J. B. *Crystalline solid electrolytes II: Material design*. In *Solid State Electrochemistry*; Bruce, P. G., Ed.; Cambridge University Press: New York, 1995; pp 43–72.

(4) Takahashi, T.; Iwahara, H.; Arao, T. *J. Appl. Electrochem.* **1975**, *5*, 187–195.

(5) Ishihara, T.; Matsuda, H.; Takita, Y. *J. Am. Chem. Soc.* **1994**, *116*, 3801–3804.

(6) Nakayama, S.; Sakamoto, M. *J. Eur. Ceram. Soc.* **1998**, *18*, 1413.

(7) Sansom, J. E. H.; Richings, D.; Slater, P. R. *Solid State Ionics* **2001**, *139*, 205–210.

(8) Ishihara, T.; Arikawa, H.; Akbay, T.; Nishiguchi, H.; Takita, Y. *J. Am. Chem. Soc.* **2001**, *123*, 203–209.

(9) Akikusa, J.; Adachi, K.; Hoshino, K.; Ishihara, T.; Takita, Y. *J. Electrochem. Soc.* **2001**, *148*, A1275–1278.

ion conductivity: 1.26×10^{-2} S/cm at 773 K).^{10–15} In this oxide, it was considered that the oxide ion can be mobile through the oxygen vacancies which are intrinsic in the double fluorite structure. This reported oxide ion conductivity is comparable with that of LaGaO₃-based oxides, and Nd₂Eu₂O₃F₆ is highly interesting because the oxide ion migrates in the fluorite-like metal oxyfluoride structure. However, the studies on oxide ion conductivity in metal oxyfluoride are limited to those close to the stoichiometric oxyfluoride composition. Because lanthanide oxyfluorides are easily decomposed in the presence of water, another problem is chemical stability. In contrast with oxyfluoride, it is known that lanthanide fluoride is stable against humidity due to the high electronegativity of fluoride.¹⁶ In this study, we focused on the oxide ion conductivity in lanthanum fluoride (LaF₃) doped with oxygen. For achieving the high oxide ion conductivity, oxygen vacancies were introduced by doping lower valence cations in the conventional study on oxides, not by doping with anions with higher valence numbers. Here, we designed oxide ion conductors that transport through oxygen doped at the anion site of LaF₃.

Experimental Section

Sample Preparation. Lanthanum fluoride used in this study was prepared by the conventional powder mixing method employing powders of La₂O₃ (Wako Pure Chemical, 99.9% in purity), LaF₃ (High Purity Chemicals, 99.9% in purity), SrF₃ (High Purity Chemicals, 99.9%), and SrCO₃ (Wako Pure Chemical, 99.9%). The amount of fluoride ion was controlled by adjusting the mixing ratio of La₂O₃ and LaF₃. Stoichiometric amounts of starting powder were weighed and mixed in an Al₂O₃ mortar with an Al₂O₃ pestle. The powder mixture was precalcined at 1023 K for 4 h in Ar gas flow (100 mL/min). After an isostatic press at 275 MPa for 20 min, the sample was finally sintered at 1273 K for 3 h in Ar gas flow.

XRD analysis of the obtained sample was performed by using a diffractometer (Rigaku Rint 2500) and a Cu K α line. After the formation of single phase LaO_xF_{3–2x} was confirmed, the disk was cut into a rectangular shape (4 mm^w \times 7 mm^L \times 1 mm^t) for the measurement of electrical conductivity.

Electrical Conductivity Measurement. Pt paste (Tanaka, TR7905) was painted on both faces of the sample, Pt mesh was connected with Pt wire attached, and then the sample was fired at 1123 K for 30 min in Ar flow. After the Pt wires were attached for the potential probe, the electrical conductivity was measured by the conventional ac two-probes technique with a frequency response analyzer (Solatron 1260) in the frequency range from 10 MHz to 1 Hz. The conductivity was also measured with the dc four-probes method, and it was noted that the conductivity estimated by both of the methods matched within an experimental error. A gas flow cell was designed to perform the oxide ionic conductivity measurements under the controlled atmosphere, maintained by using mixtures of N₂–O₂, CO–CO₂, and H₂–H₂O. The oxygen partial pressure was monitored by using a CaO-stabilized ZrO₂ oxygen sensor placed in close proximity of the specimen. The dc

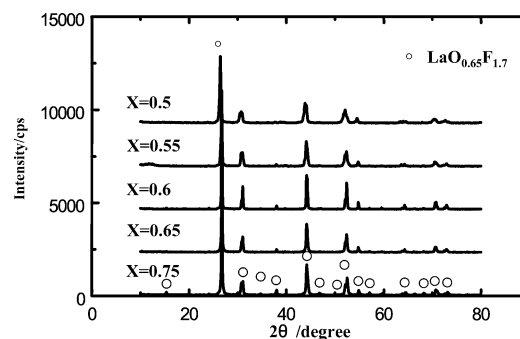


Figure 1. XRD patterns of the LaO_xF_{3–2x} prepared in this study.

polarization measurement was performed by using the same setup of conductivity measurement, and the constant dc current of 2.5 mA/cm² was applied over 24 h in N₂ atmosphere by using a galvanostat (Hokuto HA301). The potential was measured with a digital multimeter (Advantest TR6421). A dc current of 17.35 mA (2.5 mA/cm²) was constantly observed over a period of 24 h. The residual change in potential was measured as a function of time. After 24 h, the sample was cooled under application of the constant dc potential of 10 mV. Subsequently, the sample was sectioned with a diamond saw and the sectioned surface was analyzed with SEM-EDX (JEOL 6700F-Oxford INCA-4).

Ionic Transport Number Measurement. The transport number of oxide ion was estimated by the ratio of measured electromotive forces (EMF) in the H₂–O₂ gas concentration cell to that estimated with the Nernst equation. Humidified H₂ (2.8 vol %) was used as the hydrogen source, and commercial oxygen was also used without any purification. The specimen disk of 0.5 mm thickness was used for the measurements, and a gold paste (Tanaka Kikinokoku Co. Ltd.) was used for the electrode (5 mm in diameter). The relative density of the used sample for EMF measurement was found to be ca. 90%. Humidified hydrogen and oxygen were fed to either face of the sample, and the gas seal was achieved by using molten Pyrex glass. To confirm the mobile ion, the dc polarization method was applied in this study.

Results and Discussion

Oxide Ion Conductivity in LaO_xF_{3–2x}. Figure 1 shows the XRD pattern of the LaO_xF_{3–2x} prepared in this study. Diffraction patterns were drastically changed by doping with oxygen in comparison with LaF₃. Although the amount of oxygen doped was much different, the diffraction patterns similar to those of oxyfluoride, LaF_{1.7}O_{0.65}, or LaOF were observed over a wide range of *x* values. In accordance with the powder diffraction database,^{17,18} the difference in the diffraction peaks from LaF_{1.7}O_{0.65} and LaOF is quite small. However, considering the weak diffraction peaks observed around 40°, the observed diffraction peaks could be assigned to the LaF_{1.7}O_{0.65} phase. This LaF_{1.7}O_{0.65} phase is formed from the LaOF phase with interstitial fluoride ion. Takashima et al.^{10,11} also assigned the double fluorite phase to the structure similar to this LaF_{1.7}O_{0.65} phase. Because it is confirmed by X-ray fluorescence (XRF) analysis that the composition of oxygen and fluorine in the resulting sample is almost the same as that of the starting mixture, evaporation of fluoride ion from the sample during sintering seems to be negligible. Con-

(10) Takashima, M.; Kano, G. *Solid State Ionics* **1987**, *23*, 99–106.

(11) Takashima, M.; Yonezawa, S.; Ukuma, Y. *J. Fluorine Chem.* **1998**, *87*, 229–234.

(12) Takashima, M. *J. Fluorine Chem.* **2000**, *105*, 249–256.

(13) Takashima, M.; Yonezawa, S.; Leblac, M. *Solid State Ionics* **2002**, *154–155*, 547–553.

(14) Takashima, M.; Yonezawa, S.; Tanioka, T.; Nakajima; Leblanc, Y. *Solid State Sci.* **2000**, *2*, 71–76.

(15) Abrahams, I.; Nelstrop, J. A. G.; Krok, F. *Solid State Ionics* **2000**, *136–137*, 61–66.

(16) Miura, N.; Hisamoto, J.; Yamazoe, N.; Kuwata, S. *Appl. Surf. Sci.* **1988**, *33–34*, 1253–1259.

(17) Inorganic Crystal Structure Data Base, File No. 89523.

(18) Powder Diffraction File, Card No. 77-0204. International Center for Diffraction Data, Newtown Square, PA, 1998.

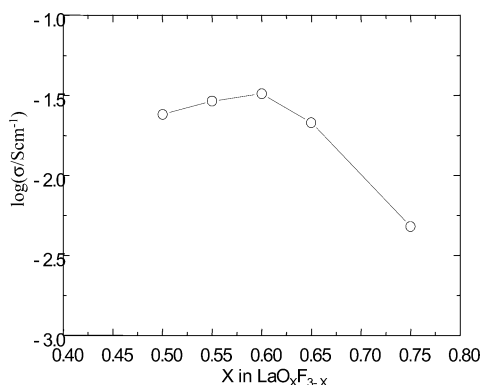
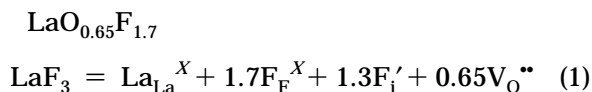


Figure 2. Electrical conductivity in LaO_xF_{3-2x} at 773 K in N₂ atmosphere as a function of *X* values.

Considering the composition, the concentration of fluoride ion is in excess of that of the LaF_{1.7}O_{0.65} phase. Therefore, it is expected that the excess fluoride ion may exist at the interstitial position, thereby introducing oxygen vacancies. With a decrease in the *X* value, the diffraction angle shifted to lower values. Thus, the lattice constant increased with an increasing amount of fluoride ion. Considering the smaller ionic radius of F⁻ (119 pm) than that of O²⁻ (126 pm), enlargement of the lattice constant can only be explained by the formation of interstitial fluoride ion. On the other hand, some weak diffraction peaks disappeared with increasing fluoride ion concentration. Therefore, the symmetry of the crystal lattice seems to be increased by increasing the F⁻ content. At *X* = 0.6, the crystal structure seems to be analogous with the oxyfluoride cubic lattice, LaOF structure. Nevertheless, all diffraction peaks can be assigned to those from lanthanum oxyfluoride, and thus the single phase was obtained over the wide range from *X* = 0.5 to 0.75 in LaO_xF_{3-2x}.

The electrical conductivity is shown in Figure 2 against the *X* value in LaO_xF_{3-2x} at 773 K in N₂ atmosphere. It is seen that the electrical conductivity increased with increasing *X* value and attained a maximum at *X* = 0.6. X-ray diffraction patterns of LaF₃ were greatly changed by doping a small amount of oxygen. As was discussed earlier, the diffraction peaks become sharp and narrow around *X* = 0.4. Thus, the crystallinity improves by doping excess fluoride ion to the LaO_{0.65}F_{1.7} phase. The amorphous phase generally exhibits low oxide ion conductivity, and normally high crystallinity and/or large grain size is required for high oxide ion conductivity. This is because the mobile ion is trapped at the grain boundary and defects. The maximum conductivity was achieved for *X* = 0.6. By an doping excess amount of fluoride ion into lanthanum oxyfluoride, we determined that oxygen vacancies will be formed by the charge compensation mode as shown below,



Therefore, it is expected that the increase in electrical conductivity is caused by the increase in ionic conductivity. Because the ionic radius of the fluoride ion is smaller than that of the oxygen ion, it is considered that

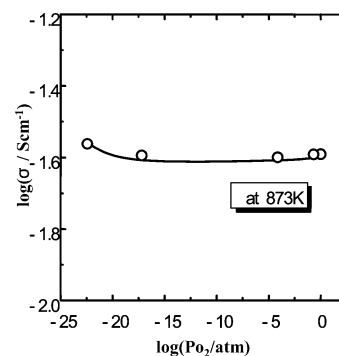


Figure 3. *P*_{O₂} dependence of the electrical conductivity in LaO_{0.6}F_{1.8} at 873 K.

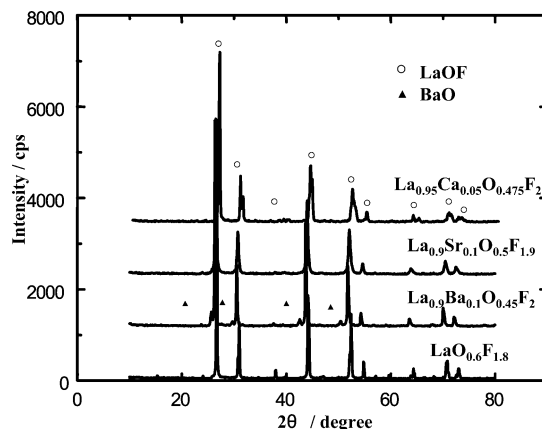


Figure 4. XRD patterns of La_{1-x}M_xO_{0.6-3/2x}F_{1.8+2x} (M = Ca, Sr, and Ba).

the lattice parameter will increase by substituting O²⁻ for F⁻. However, the lattice volume is also increased by increasing the oxygen deficiency. This could only be explained by the introduction of anion vacancies and interstitial F⁻ ions. In any case, the crystal symmetry changed from orthorhombic to cubic or pseudo-cubic structure, which is close to the LaOF structure, and the conductivity may be either oxide or fluoride ion conductivity.

To confirm the ionic conductivity, the *P*_{O₂} dependence of the electrical conductivity was measured for LaO_{0.6}F_{1.8} (Figure 3). As expected, the electrical conductivity of LaO_{0.6}F_{1.8} was independent of the oxygen partial pressure up to 10⁻¹⁷ atm at 873 K. However, the electrical conductivity slightly increased in H₂ atmosphere (*P*_{O₂} = 10⁻²³ atm), suggesting the appearance of electronic conduction. However, it is seen that the ion conductivity is dominant in LaO_{0.6}F_{1.8} oxide over a wide *P*_{O₂} range, because the increase in conductivity in H₂ atmosphere is not large.

Effects of Dopant on Ion Conductivity in LaO_{0.6}F_{1.8}. The effects of aliovalent cation doping for the La site in LaO_{0.6}F_{1.8} were further investigated. In the case of the conventional oxide ion conductor, the addition of lower valence cations is generally essential for achieving fast oxide ion conductivity. Figure 4 shows the XRD patterns of La_{1-x}M_xO_{0.6-3/2x}F_{1.8+2x} (M = Ca, Sr, and Ba). As is shown in Figure 4, the XRD measurement suggests that the secondary phase of BaO was formed, but no secondary phase was observed for the Ca- and Sr-doped sample. Therefore, the solubility of Ba²⁺ into LaF₃ lattice is not high due to the large ionic

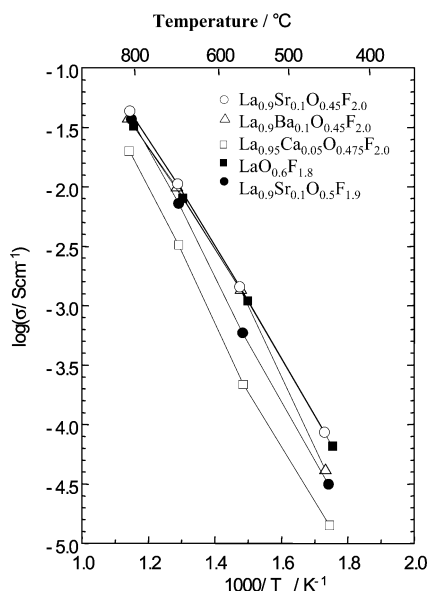
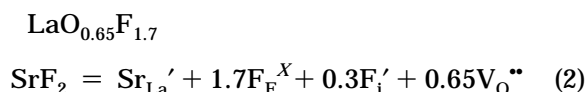


Figure 5. Temperature dependence of the electrical conductivity of $\text{La}_{1-x}\text{M}_x\text{O}_{0.6-3/2x}\text{F}_{1.8+2x}$ ($\text{M} = \text{Ca}, \text{Sr}, \text{and Ba}$) and $\text{La}_{0.9}\text{Sr}_{0.1}\text{O}_{0.5}\text{F}_{1.9}$.

size of Ba^{2+} . However, except for BaF_2 , all diffraction peaks can be assigned to those from oxygen-doped LaF_3 . In addition, main diffraction peaks were also shifted by doping CaF_2 . Therefore, it is seen that SrF_2 or CaF_2 substituted the La site in the LaF_3 lattice. Because the ionic size of Ca^{2+} is much smaller than that of La^{3+} , diffraction peaks from LaF_3 doped with CaF_2 were split into two, suggesting that the crystal structure changes from cubic to tetragonal structure.

The temperature dependence of electrical conductivity in $\text{La}_{1-x}\text{M}_x\text{O}_{0.6-3/2x}\text{F}_{1.8+2x}$ ($\text{M} = \text{Ca}, \text{Sr}, \text{and Ba}$) is shown in Figure 5. Due to the phase change, the electrical conductivity of $\text{LaO}_{0.6}\text{F}_{1.8}$ decreased by doping CaF_2 ; however, it slightly increased by doping SrF_2 and BaF_2 at high temperature, albeit it decreased at low temperature. Because the formation of a secondary phase was observed, it can be considered that SrF_2 is the most effective as the dopant. Considering equation (2), doping SrF_2 to $\text{LaO}_{0.6}\text{F}_{1.8}$ enlarges the relative concentration of fluoride ion and reduces that of oxygen. Hence, the interstitial fluoride ion and the oxygen vacancy increased as described by the following equation,



If the interstitial fluoride ion is the mobile species, then the electrical conductivity should increase by doping SrF_2 . Indeed, the electrical conductivity increased by doping SrF_2 ; however, the increase in conductivity is not large as is shown in Figure 5. On the other hand, if the oxide ion conductivity appeared, then it is also considered that the ionic conductivity increases because of the formation of oxygen vacancy. However, considering that the amount of charge carrier of oxygen decreases by substitution with SrF_2 , an increase in conductivity may not be large enough. In any case, it is seen that the optimum amount of SrF_2 doped for LaF_3 exists at ca. 10 mol %.

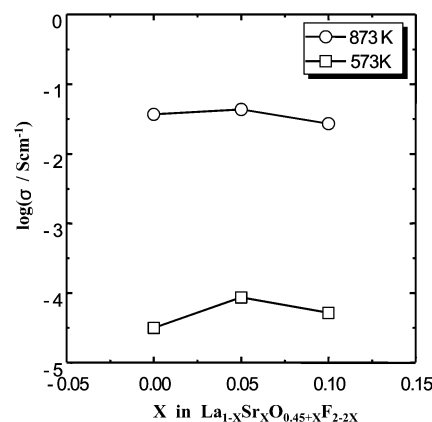


Figure 6. Electrical conductivity in $\text{La}_{0.9}\text{Sr}_{0.1}\text{O}_{0.45+X}\text{F}_{2-2X}$ as a function of the X value.

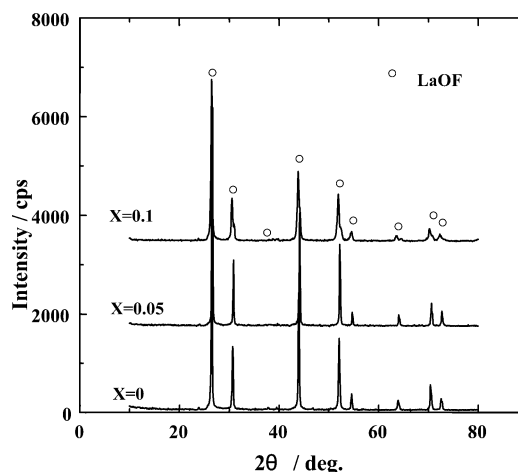
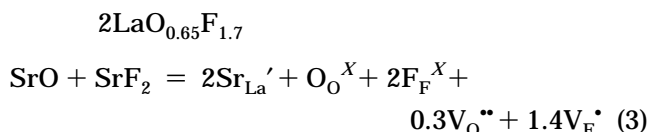


Figure 7. XRD patterns of $\text{La}_{0.9-x}\text{Sr}_{0.1}\text{Na}_x\text{O}_{0.5-2x}\text{F}_{2.0+2x}$.

Because the doping of strontium fluoride decreases the amount of oxygen in the lattice, co-doping of strontium oxide and fluoride was also tried to keep the oxygen amount constant. As expected, conductivity increased by co-doping a small amount of strontium oxide and fluoride as shown in Figure 6. In particular, improvement in conductivity is significant at lower temperature. Therefore, it becomes clear that the doping of a small amount of strontium oxide is effective for increasing the electrical conductivity in lanthanum fluoride. Co-doping of strontium oxide and fluoride could be explained by the equation (3),



Because the amount of charge carrier oxygen could remain high according to equation (3) and oxygen vacancy was introduced, the oxide ion conductivity increases by co-doping oxide and fluoride. Indeed, the highest electrical conductivity was achieved for $\text{La}_{0.9}\text{Sr}_{0.1}\text{O}_{0.5}\text{F}_{1.9}$.

The influences of doping alkaline fluoride on the electrical conductivity were further studied. Figure 7 shows the XRD patterns of the sample doped with NaF . XRD measurement suggests that the doped NaF successfully substitutes the lattice position of the LaF_3 crystal. This is because the diffraction angle was shifted

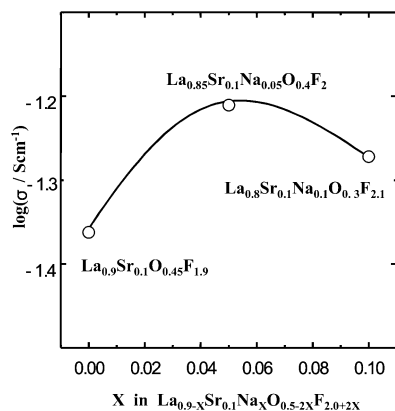
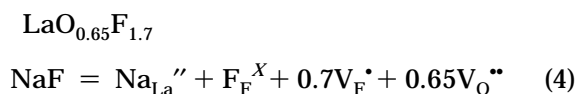


Figure 8. Electrical conductivity of $\text{La}_{0.9-x}\text{Sr}_{0.1}\text{Na}_x\text{O}_{0.5-2x}\text{F}_{2.0+2x}$ at 873 K as a function of the x value.

to a lower angle by doping NaF. Because the ionic size of Na^+ (98 pm) is smaller than that of La^{3+} (126 pm), NaF substitutes at the LaF_3 lattice position to form an anion vacancy according to the following equation,



Because of the decrease in the negative charge and the increase in anion vacancy, it can be considered that decreasing coulomb efficiency enlarged the lattice constant. Therefore, doping NaF is effective for increasing the oxide ion conductivity.

Figure 8 shows the electrical conductivity at 873 K as a function of the NaF dopant amount. It is seen that the electrical conductivity increased with an increase in the amount of NaF and it attained the maximum value around 5 mol % to the La site. Because the amount of oxygen becomes smaller with an increase in the amount of NaF as dopant, the excess amount of NaF is not desirable. In the present case, the optimized amount for NaF addition exists at a value as small as 5 mol %.

If the main charge carrier is ion, the electronic conductivity should be independent of oxygen partial pressure. However, if the electronic conduction is dominant, then the conductivity should increase or decrease as the oxygen partial pressure (P_{O_2}) increases. To confirm the ionic conductivity in this doubly doped lanthanum oxyfluoride compound, P_{O_2} dependence of the electrical conductivity was measured for $\text{La}_{0.85}\text{Sr}_{0.1}\text{Na}_{0.05}\text{O}_{0.4}\text{F}_{2.0}$, and the results are shown in Figure 9. Obviously, the electrical conductivity of $\text{La}_{0.85}\text{Sr}_{0.1}\text{Na}_{0.05}\text{O}_{0.4}\text{F}_{2.0}$ was independent of the oxygen partial pressure over a wide range of P_{O_2} (from 1 to 10^{-21} atm) at 873 K. As compared with the P_{O_2} dependence in Figure 3, it is clear that the P_{O_2} range for ion conductivity expanded with NaF doping. This is generally caused by the increase in ion conductivity. Therefore, doping SrF_2 , SrO , and NaF is effective for increasing the ion conductivity, and it is obvious that this ionic conductivity is dominant in $\text{La}_{0.85}\text{Sr}_{0.1}\text{Na}_{0.05}\text{O}_{0.4}\text{F}_{2.0}$ over a wide P_{O_2} range.

Identification of Charge Carrier and Chemical Stability of Doped Lanthanum Oxyfluoride. To confirm the mobile ion species in Sr-, Na-, and O-doped LaF_3 , the ionic transport number was estimated by

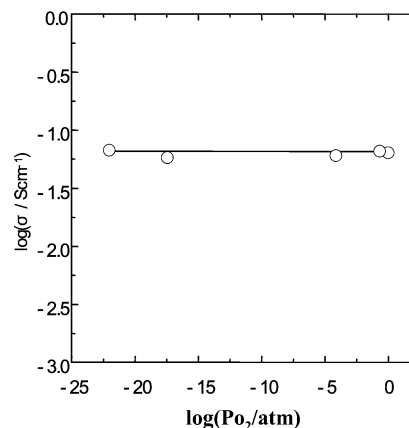


Figure 9. P_{O_2} dependence of the electrical conductivity of $\text{La}_{0.85}\text{Sr}_{0.1}\text{Na}_{0.05}\text{O}_{0.4}\text{F}_{2.0}$ at 873 K.

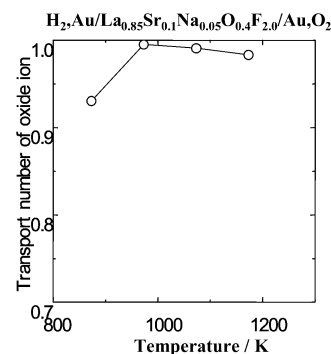


Figure 10. Temperature dependence of the electromotive force (EMF) for a humidified H_2 – O_2 gas concentration cell using $\text{La}_{0.85}\text{Sr}_{0.1}\text{Na}_{0.05}\text{O}_{0.4}\text{F}_{2.0}$ as the electrolyte.

using the oxygen gas concentration cell. Figure 10 shows the temperature dependence of the electromotive force (EMF) for the humidified H_2 and O_2 gas concentration cell. It is seen that the EMF measurement shows a value higher than 90% of the theoretical value by assuming the oxide ion conductivity at all temperatures examined. Therefore, it is expected that the dominant ionic charge carrier in $\text{La}_{0.9}\text{Sr}_{0.1}\text{Na}_{0.05}\text{O}_{0.4}\text{F}_{2.0}$ is the oxide ion. To further clarify the oxide ion conductivity, a polarization measurement was performed under the application of constant dc current on $\text{La}_{0.9}\text{Sr}_{0.1}\text{O}_{0.5}\text{F}_{1.9}$. If the fluoride ion conductivity is dominant, it is expected that the conductivity decrease with the time course when the constant dc current is applied. Furthermore, fluoride accumulation will be observed at the positive electrode side.

Figure 11 shows the conductivity under application of a constant dc current of 2.5 mA/cm². It is clear that the constant conductivity was observed over ca. 24 h. In addition, the electrical conductivity measured by the ac impedance method was also superimposed on this figure. It is seen that the observed conductivity by the dc polarization condition is almost the same as that of the ac impedance method. Therefore, it can be confirmed that the oxide ion conductivity is dominant and fluoride ion conductivity is negligible at 773 K in $\text{La}_{0.9}\text{Sr}_{0.1}\text{O}_{0.5}\text{F}_{1.9}$.

Figure 12 shows the SEM observation and the X-ray line analysis of the F and O $K\alpha$ line. Because the intensity of the X-ray emission is strongly influenced by the geometrical morphology of the specimens, the X-ray line was slightly scattered. However, it is seen that there is no significant enhancement in the intensity

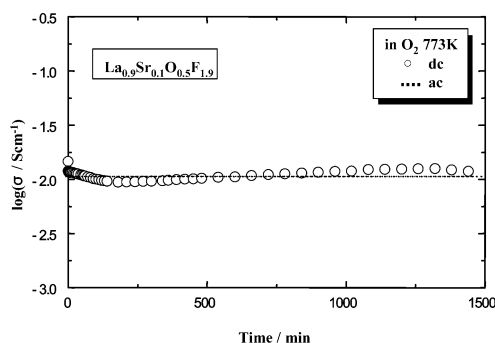


Figure 11. Electrical conductivity in $\text{La}_{0.9}\text{Sr}_{0.1}\text{O}_{0.5}\text{F}_{1.9}$ estimated by the dc four-probes method as a function of time.

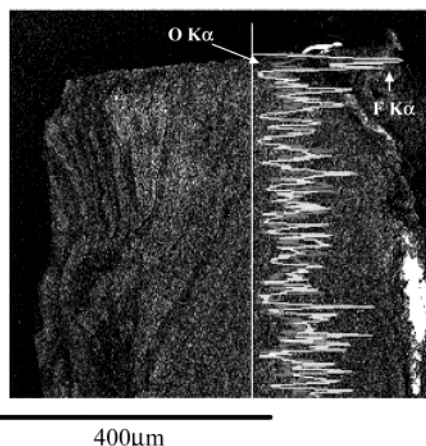


Figure 12. SEM observation and the X-ray line analysis of the F and O $K\alpha$ line on $\text{La}_{0.9}\text{Sr}_{0.1}\text{O}_{0.5}\text{F}_{1.9}$.

Table 1. Comparison of the Amount of Trapped Fluoride Ion with That Estimated by Assuming F^- Ion Conductor during dc Polarization Measurement^a

amount of F^- ion assumed by F^- ion conductor/mol	amount of F^- ion trapped by cold water/mol	ratio
2.24×10^{-3}	1.03×10^{-5}	0.0045

^a dc polarization: 2.5 mA, 48 h.

of the F and O $K\alpha$ X-ray line. Because the constant potential was applied during the cooling cycle, it can be said that no anion remixing occurred during cooling. Hence, there is no accumulation of fluoride and oxygen at the positive electrode side. These results suggest clearly that the charge carrier in this lanthanum oxyfluorite is oxide ion.

To confirm the remixing effects of oxygen and fluoride ion, fluorine which was desorbed during the dc polarization measurement was trapped by cold water, and the amount of fluorine was compared with the coulomb number passed. As is shown in Table 1, a small amount of fluorine was formed during the dc polarization measurement for 24 h. However, as compared with the total current passed, the amount of trapped fluorine is just 0.45% against the total coulomb number. This also confirmed that the main charge carrier is oxide ion and not fluoride ion in doped lanthanum oxyfluorite. As was discussed before, some of the fluoride ion seems to exist at the interstitial position; however, this interstitial fluoride ion seems not to be mobile. A similar result was also reported for double lanthanum oxyfluoride by Takashima et al.¹¹ Consequently, it can be confirmed that the oxide ion is the dominant mobile ion species

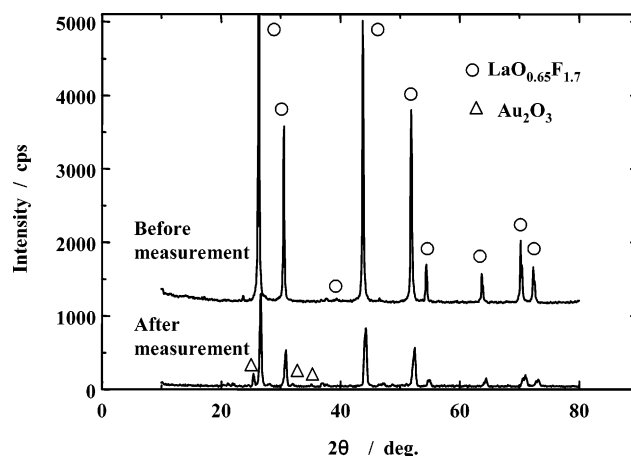


Figure 13. XRD patterns of $\text{La}_{0.9}\text{Sr}_{0.1}\text{O}_{0.5}\text{F}_{1.9}$ before and after measurement of EMF for the $\text{H}_2\text{--H}_2\text{O/O}_2$ gas concentration cell.

and the fluoride ion is the minor charge carrier in $\text{La}_{0.9}\text{Sr}_{0.1}\text{O}_{0.5}\text{F}_{1.9}$ and in $\text{La}_{0.85}\text{Sr}_{0.1}\text{Na}_{0.05}\text{O}_{0.4}\text{F}_{2.0}$.

It is well-known that lanthanum oxyfluoride is not stable against water and lanthanum oxyhydroxide is easily formed. Because the formation of a small amount of fluorine was also observed during the dc polarization measurement, the chemical stability of doped lanthanum oxyfluoride was also studied. Table 1 also shows the amount of F^- ion eluted from $\text{La}_{0.9}\text{Sr}_{0.1}\text{O}_{0.5}\text{F}_{1.9}$ for 240 h when the sample was drenched in deionized water. A small amount of fluoride ion was eluted from the sample by drenching in water. However, the total amount of eluted fluoride ion was just 0.008% in the sample for 4 days, and no change in XRD was observed after drenching in water for 4 days. Therefore, it can be said that $\text{La}_{0.9}\text{Sr}_{0.1}\text{O}_{0.5}\text{F}_{1.9}$ is highly stable against water at room temperature.

The high-temperature stability of the sample against humidity was also checked. Figure 13 shows the XRD patterns of $\text{La}_{0.9}\text{Sr}_{0.1}\text{O}_{0.5}\text{F}_{1.9}$ before and after measurement of EMF for the $\text{H}_2\text{--H}_2\text{O/O}_2$ gas concentration cell. It was noticed that EMF almost corresponds to the theoretical value (as shown in Figure 10) that was sustained over 24 h against humidified hydrogen, albeit a small increase in EMF is observed. No change in XRD patterns was observed before and after exposure to humidified H_2 for 24 h. Therefore, it can be considered that the chemical stability of $\text{La}_{0.9}\text{Sr}_{0.1}\text{O}_{0.5}\text{F}_{1.9}$ against humidity is high enough for the electrolyte of solid oxide fuel cells not only at low temperature but also at intermediate temperature around 673 K.

Figure 14 shows the comparison of the oxide ion conductivity in $\text{La}_{0.85}\text{Sr}_{0.1}\text{Na}_{0.05}\text{O}_{0.4}\text{F}_{2.0}$ and that in the conventional fluorite and perovskite structured oxide. It is seen that the oxide ion conductivity in $\text{La}_{0.85}\text{Sr}_{0.1}\text{Na}_{0.05}\text{O}_{0.4}\text{F}_{2.0}$ is much higher than that of the commonly used oxide ion conductors such as Y_2O_3 -stabilized ZrO_2 , CeO_2 -doped Sm, or LaGaO_3 -based oxide. Even as compared with the binary rare-earth oxide-fluoride of $\text{Nd}_2\text{--Eu}_2\text{O}_3\text{F}_6$, which was reported as the highest oxide ion conductor in oxyfluoride, LaF_3 doped with Sr, Na, and O shows higher conductivity. In addition, as is shown in Figure 9, the oxide ion conductivity is stably exhibited over a wide P_{O_2} range and even in wet atmosphere. Consequently, Na- and Sr-doped lanthanum oxyfluorite

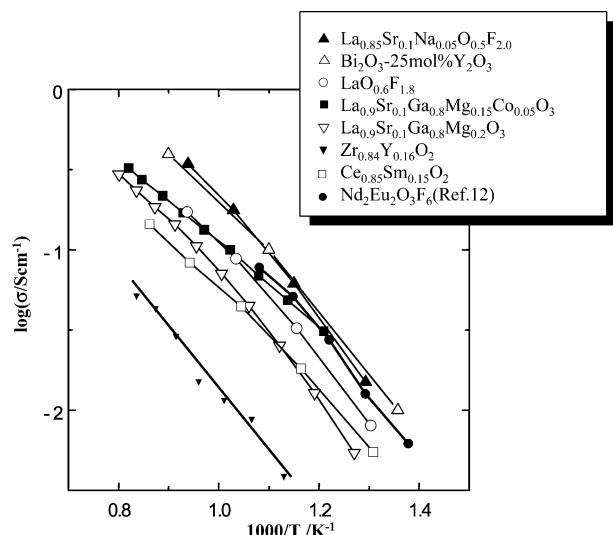


Figure 14. Comparison of oxide ion conductivity in the conventional oxides with that in $\text{La}_{0.85}\text{Sr}_{0.1}\text{Na}_{0.05}\text{O}_{0.4}\text{F}_{2.0}$.

is a highly interesting material as the oxide ion-conducting electrolyte for low-temperature-operating solid oxide fuel cells.

Conclusion

In this study, a new class of oxide ion conductors was developed on the basis of the concept that the doped oxygen can be mobile in lattice. It is considered that this

concept can be applied to a wider range of compounds such as nitrides and carbides. There is a large possibility that a new class of fast oxide ion conductors will be developed on the basis of this material design. Due to high chemical stability, we believe that Sr-, Na-, and O-doped LaF_3 is highly attractive as a new oxide ion conductor for various applications, in particular, as the electrolyte of solid oxide fuel cells. The highest conductivity was achieved at $\text{La}_{0.9}\text{Sr}_{0.1}\text{Na}_{0.05}\text{O}_{0.4}\text{F}_{2.0}$ in this study. Also, this compound is chemically stable in oxygen partial pressure from 1 to 10^{-21} atm. The theoretical electromotive forces were almost exhibited on the oxygen gas-concentration cell. The polarization measurement confirmed that the oxide ion conductivity is dominant in $\text{La}_{0.9}\text{Sr}_{0.1}\text{Na}_{0.05}\text{O}_{0.4}\text{F}_{2.0}$. The oxide ion conductivity in $\text{La}_{0.85}\text{Sr}_{0.1}\text{Na}_{0.05}\text{O}_{0.4}\text{F}_2$ is much higher than that of the commonly used oxide ion conductors such as Y_2O_3 -stabilized ZrO_2 , CeO_2 doped with Sm, or LaGaO_3 doped with Sr and Mg. In comparison with that of the binary rare-earth oxide-fluoride of $\text{Nd}_2\text{Eu}_2\text{O}_3\text{F}_6$, the electrical conductivity of $\text{La}_{0.85}\text{Sr}_{0.1}\text{Na}_{0.05}\text{O}_{0.4}\text{F}_2$ is higher. Consequently, $\text{La}_{0.9}\text{Sr}_{0.1}\text{Na}_{0.05}\text{O}_{0.4}\text{F}_{2.0}$ is highly attractive as a new class of oxide ion conductor.

Acknowledgment. We acknowledge the financial support from a Grant-in-Aid for Science Promotion (No. 11102006) from the Ministry of Education, Culture, Sports, Science, and Technology of Japan.

CM049186H